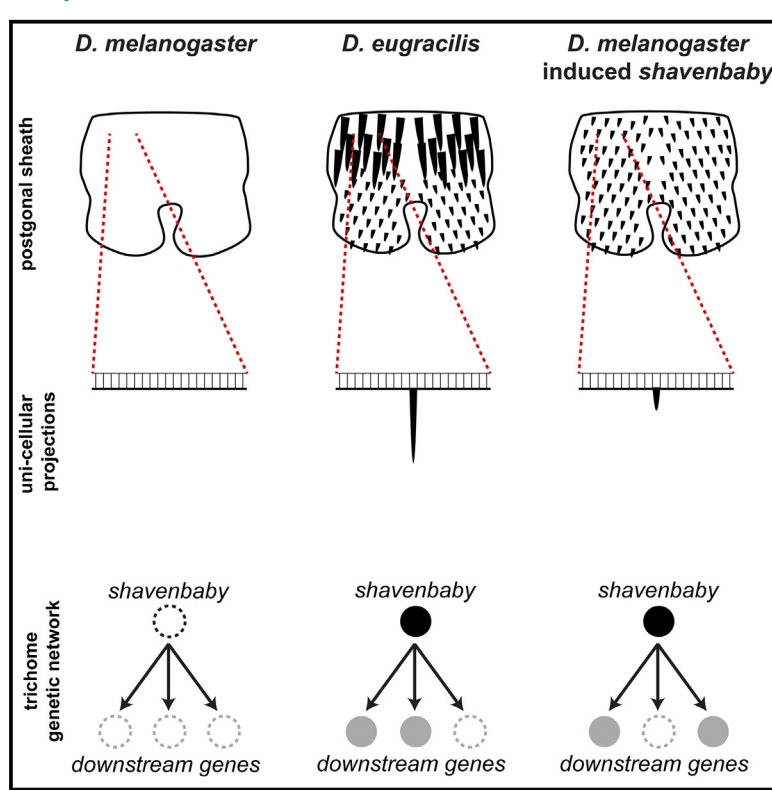
Current Biology

Co-option of the trichome-forming network initiated the evolution of a morphological novelty in Drosophila eugracilis

Graphical abstract



Authors

Gavin Rice, Tatiana Gaitán-Escudero, Kenechukwu Charles-Obi, Julia Zeitlinger, Mark Rebeiz

Correspondence

grr24@pitt.edu (G.R.), rebeiz@pitt.edu (M.R.)

In brief

Rice et al. show that novel unicellular projections found in the postgonal sheath of *Drosophila eugracilis* express the key trichome transcription factor *shavenbaby* and 14 genes of the known larval trichome genetic network. Expression of *shavenbaby* in the projection-lacking species *Drosophila melanogaster* is sufficient to induce this novel trait.

Highlights

- Unicellular projections of the *D. eugracilis* postgonal sheath express shavenbaby
- The D. eugracilis projections co-opted a portion of the larval trichome GRN
- shavenbaby misexpression recapitulates short projections in D. melanogaster
- Upon co-option, the GRN was specialized to produce diverse projection morphologies









Article

Co-option of the trichome-forming network initiated the evolution of a morphological novelty in *Drosophila eugracilis*

Gavin Rice, 1,* Tatiana Gaitán-Escudero, 2 Kenechukwu Charles-Obi, 1 Julia Zeitlinger, 2,3 and Mark Rebeiz 1,4,5,*

- ¹Department of Biology, University of Pittsburgh, Pittsburgh, PA 15260, USA
- ²Stowers Institute for Medical Research, Kansas City, MO 64110, USA
- ³Department of Pathology and Laboratory Medicine, The University of Kansas Medical Center, Kansas City, KS 66160, USA
- ⁴X (formerly Twitter): @RebeizLab
- ⁵Lead contact

 ${}^{\star}\text{Correspondence: } \underline{\text{grr24@pitt.edu (G.R.), rebeiz@pitt.edu (M.R.)}}$

https://doi.org/10.1016/j.cub.2024.09.073

SUMMARY

Identifying the molecular origins by which new morphological structures evolve is one of the long-standing problems in evolutionary biology. To date, vanishingly few examples provide a compelling account of how new morphologies were initially formed, thereby limiting our understanding of how diverse forms of life derived their complex features. Here, we provide evidence that the large projections on the Drosophila eugracilis phallus that are implicated in sexual conflict have evolved through the partial co-option of the trichome genetic network. These unicellular apical projections on the phallus postgonal sheath are reminiscent of trichomes that cover the *Drosophila* body but are up to 20-fold larger in size. During their development, they express the transcription factor Shavenbaby, the master regulator of the trichome network. Consistent with the co-option of the Shavenbaby network during the evolution of the D. eugracilis projections, somatic mosaic CRISPR-Cas9 mutagenesis shows that shavenbaby is necessary for their proper length. Moreover, misexpression of Shavenbaby in the sheath of D. melanogaster, a naive species that lacks these projections, is sufficient to induce small trichomes. These induced projections rely on a genetic network that is shared to a large extent with the D. eugracilis projections, indicating its partial co-option but also some genetic rewiring. Thus, by leveraging a genetically tractable evolutionary novelty, our work shows that the trichome-forming network is flexible enough that it can be partially co-opted in a new context and subsequently refined to produce unique apical projections that are barely recognizable compared with their simpler ancestral beginnings.

INTRODUCTION

The mystery surrounding morphological novelties lies in the inherent difficulty of explaining their evolutionary origins. One proposed mechanism for initiating a novel morphological structure is the redeployment of an established gene regulatory network (GRN) to a new developmental context. 1-4 Such GRN co-option is thought to result from the recruitment of one or a few top-tier regulators within a network to a tissue that previously lacked expression.^{5,6} The mechanism of GRN redeployment has been extensively studied in the field of evolutionary development. It has been implicated across many species⁷⁻⁹ in many different contexts¹⁰⁻¹⁴ and is often linked by shared gene co-expression patterns, pleiotropic enhancer elements, and pleiotropic effects of gene perturbations. 15-19 While perturbations of many genes of a GRN may disrupt a phenotype, a very small number of genes will be sufficient to induce the phenotype in naive tissues.^{5,6} These novelty-inducing factors have therefore remained elusive because of their relative scarcity within GRNs and the lack of genetic tools in many species that bear novel traits of interest. Inducing a novelty

genetically would allow us to probe the nascent stages of genetic network co-option and examine how subsequent rounds of evolutionary refinement may have proceeded.^{1,20}

Across animals, reproductive structures are some of the most diverse and rapidly evolving morphological traits.²¹⁻²³ For this reason, they are excellent candidates for genetic and developmental investigations of novel traits. As an example, diverse genital morphologies are present in species of Drosophila, and the rapid pace of genital evolution has often been attributed to conflict between the sexes. 21,22,24 Drosophila eugracilis, which is a member of the sister group to the *melanogaster* subgroup, ^{25–27} shows a unique set of outgrowths covering the surface of the phallus.²³ The adult postgonal sheath (also known as the aedeagal sheath²⁸) of *D. eugracilis* is covered with over 150 differently sized projections, which have been implicated in copulatory wounding to facilitate the entry of male seminal proteins into the female circulatory system, increasing ovulation and reducing remating rates^{23,29} (Figure 1). The recent origin of these projections makes them an ideal model for investigating the genetics behind complex morphological novelties.





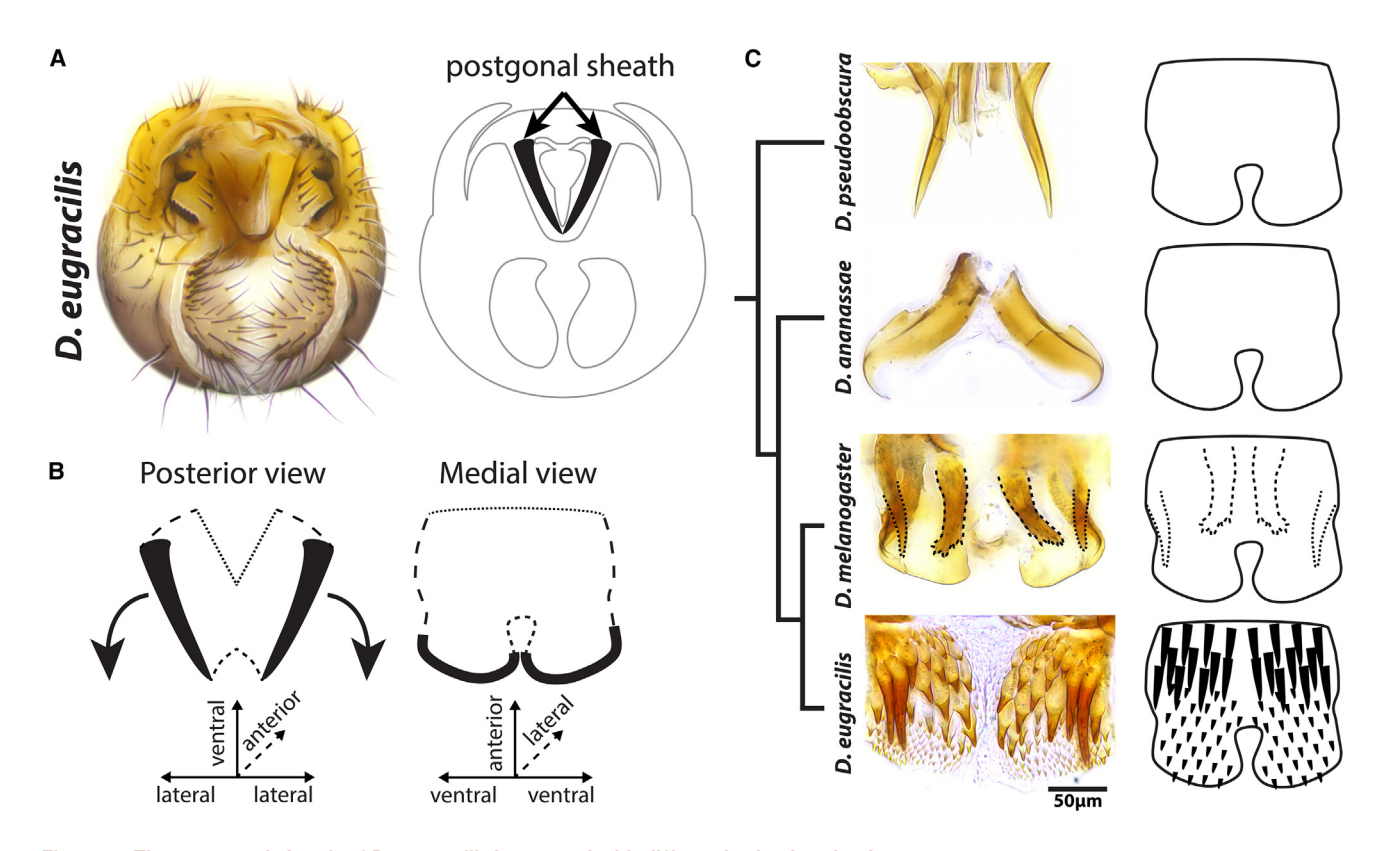


Figure 1. The postgonal sheath of D. eugracilis is covered with differently sized projections

(A) Left: light microscopy images of the *D. eugracilis* adult male terminalia (genitalia and analia). Right: a schematic representation of the *D. eugracilis* adult terminalia, highlighting the position of the postgonal sheath.

(B) A schematic representation of the adult postgonal sheath. Left: posterior view of the postgonal sheath, orientation seen while attached to the whole terminalia. Right: medial view of the postgonal sheath, orientation seen once dissected and flattened for imaging.

(C) Medial view of the adult postgonal sheath. Left: light microscopy images of *D. pseudoobscura* (top), *D. ananassae*, *D. melanogaster*, and *D. eugracilis* (bottom) postgonal sheaths. The *D. melanogaster* postgonal sheath contains two pairs of multicellular outgrowths: the ventral postgonal process (small dotted outline) and dorsal postgonal process (large dotted outline). The *D. eugracilis* postgonal sheath is covered with over 150 projections. Right: schematic representations of the *D. melanogaster* and *D. eugracilis* postgonal sheaths. Corresponding images of the *D. eugracilis* female genitalia can be found in Figure S1. Scale bar, 50 µm.

Although the genetic network of the D. eugracilis postgonal sheath projections had not been previously studied, the GRN that controls the D. melanogaster larval hairs (also known as trichomes) is one of the most thoroughly characterized genetic networks in the literature. 30-32 The transcription factor genes shavenbaby (svb) and SoxNeuro (SoxN) are necessary for trichome development, as evidenced by the loss or large reduction in the height of trichomes in the larvae as well as in the adult wings, legs, and abdomens in svb mutants. 33-36 These two transcription factors bind many of the same genes involved in trichome development but also independently regulate some members of the trichome genetic network.³⁷ Over 150 genes are direct targets of Svb in the larval trichomes, including genes that contribute to actin bundling and extracellular matrix (ECM) formation. 38,39 The loss of svb expression has been found to be the key evolutionary change underlying the independent loss of the dorsal larval trichomes in several species of Sophophora, indicating that it is a key gene in this network.⁴⁰⁻⁴³ Furthermore, it has been shown that svb and SoxN are capable of inducing larval trichomes in cells that do not normally produce them.37 Finally, the trichome types of the larvae (dorsal and ventral) also have unique morphologies, with the ventral

trichomes showing a darkly pigmented saw tooth morphology while the dorsal type 4 trichomes are less pigmented and have a thinner shape. ⁴⁴ Despite the creative potential of the trichome network, studies of trichome evolution have necessarily focused on loss, and the genes that cause the unique morphologies of different trichomes have not been well established.

To investigate the genetic network involved in the postgonal sheath projections of D. eugracilis, we analyzed their development, both morphologically and molecularly. We found that they are produced by unicellular apical outgrowths similar to larval trichomes. Both svb and SoxN were expressed in the D. eugracilis postgonal sheath, and a large portion of the larval trichome genetic network is species-specifically expressed. Of note, we show that the misexpression of svb in the postgonal sheath of D. melanogaster is sufficient to recapitulate small projections reminiscent of the D. eugracilis novel projections. Comparing the induced trichomes of D. melanogaster to the novel trichomes of D. eugracilis identifies a core portion of the trichome network shared between larvae and genital contexts. Our work provides a glimpse at the incipient stages of novelty and highlights the challenges of exploring the subsequent steps of elaboration.





RESULTS

Comparative anatomy of *D. eugracilis* and *D. melanogaster* genital traits

To visualize the stereotyped positions and connectivity of the D. eugracilis projections, we performed microdissections of the D. eugracilis phallus (Figures 1A and 1B). All projections are directly connected to the postgonal sheath (also known as the aedeagal sheath²⁸), an epithelial tissue produced from the genital disc. The anterior portion of the D. eugracilis postgonal sheath produces large projections, while the posterior portion produces smaller projections (Figure 1C). Our previous analysis found that the postgonal sheaths of the eight members of the melanogaster, suzukii, and ananassae subgroups have smooth medial surfaces without detectable projections,²⁴ similar to the morphology of the more basal D. pseudoobscura (Figure 1C). The D. melanogaster postgonal sheath produces four large multicellular spine-like structures,24 known as the postgonal processes (also known as the postgonites²⁸). These large multicellular spines in D. melanogaster are similar in size and shape to the largest projections we find in the D. eugracilis postgonal sheath. The female external genitalia of D. eugracilis are similar in morphology to D. melanogaster, 45 while the internal genitalia (vagina) potentially show a pleated morphology and contain many hair-like structures known as trichomes⁴⁶ (Figure S1).

The D. eugracilis projections are unicellular

To investigate possible genetic mechanisms that generated the D. eugracilis projections, we first examined how they develop. We initially tested if the *D. eugracilis* projections were produced by multicellular outgrowths similar to the D. melanogaster postgonal processes. To visualize the phallic morphology macroscopically, we employed ECAD antibody staining (which highlights apical cellular junctions), revealing that the D. eugracilis pupal phallus at 48 h after pupal formation (APF) did not show any multicellular outgrowths (Figures 2E and 2E'). This led us to test if these projections could instead be produced by unicellular outgrowths. Other well-characterized unicellular projections (such as larval trichomes) form actin-rich projections from the cell's apical surface. 47 Co-staining ECAD and phalloidin (which highlights actin) in the developing postgonal sheath of D. eugracilis revealed actin-rich apical projections that each extend from a single cell. These unicellular projections cover the medial postgonal sheath where the projections of the adult are found (Figure 2G'). The unicellular projections begin forming at 44 h APF, similar to when trichomes start forming in the pupal abdominal epidermis⁴⁸ and are close to their adult size at 52 h APF (Figure S2). ECAD/phalloidin co-staining of D. melanogaster postgonal sheaths did not show unicellular projections. However, unicellular projections are also found on the aedeagus, medium gonocoxite, and dorsal postgonal process (Figures 2C and S3). The lack of unicellular projections in the postgonal sheath of D. melanogaster suggests that the unicellular projections in the D. eugracilis postgonal sheath likely represent a novelty.

The *D. eugracilis* postgonal sheath projections are modified trichomes

Since the unicellular projections of the *D. eugracilis* postgonal sheath developed similar to unicellular larval trichomes of

Drosophila, we investigated whether the key transcription factor, svb, also known as ovo (FBgn0003028), was involved. We established an antibody for svb that has binding specificity in both D. melanogaster and D. eugracilis. As a positive control, we show that it correctly stains the 12 h after egg laying embryotic pattern (Figure S4). Antibody staining and in situ hybridization in the developing D. eugracilis phallus revealed that svb was expressed in the postgonal sheath where the unicellular projections are found and revealed that the anterior regions of the postgonal sheath, which house the largest projections, contain large nuclei (Figures 2I and 2J). Expression of svb is first observed at 44 h APF when unicellular projections begin to form and continues until 52 h APF (Figure S2). The same analysis for the phallus of D. melanogaster at 48 h APF did not detect svb expression in the postgonal sheath (Figures 2G and 2H). Thus, the gain of svb expression in the medial postgonal sheath is correlated with the gain of unicellular projections. Expression of svb was found in the D. melanogaster aedeagus, medium gonocoxite, and dorsal postgonal process (Figure 2J), which corresponds to the unicellular projections we see in these regions. This indicates that the processes of the postgonal sheath are modified trichomes, and we will refer to them as postgonal sheath trichomes throughout the remainder of the text.

We next tested whether the cellular effectors of the larval trichome GRN were expressed in the postgonal sheath of D. eugracilis. We examined the expression of 23 known larval trichome GRN cellular effectors 38,39,49 in the D. eugracilis postgonal sheath 48 h APF by in situ hybridization (Figure 3). Fourteen out of 23 tested cellular effectors show strong expression in the medial postgonal sheath, while 9 genes did not show strong expression (Figure S5; Table S1). The majority of ECM and actin cellular effectors are expressed in the medial postgonal sheath. Although not all of the larval trichome genetic network showed expression in the postgonal sheath, variation is also seen between larval trichomes. 38,39,49 Dorsal larval trichomes express 21 out of 23 of the genes we analyzed, while the ventral trichomes express 22 out of 23 (Table S2). Additionally, the D. eugracilis medium gonocoxite, which also houses trichomes, expresses 50% of the larval trichome GRN that we analyzed (Figure S5; Table S5). It is also possible that these undetected genes are expressed at a different developmental stage than the one we surveyed. The localized expression of svb and 14 cellular effectors in the D. eugracilis medial postgonal sheath indicates that a substantial portion of the larval trichome genetic network is present in these novel structures.

svb is necessary for the largest postgonal sheath trichomes of *D. eugracilis*

We next wanted to determine the necessity of svb for the *D. eugracilis* postgonal sheath trichome morphology. Null mutations of svb have been shown to reduce the height or even lead to the loss of larval, leg, abdominal, and wing trichomes. ^{33–37} We tested this by inducing Cas9-mediated mosaic mutants (Figure 4B). ⁵⁰ In brief, this technique involves injecting pre-cellularized embryos with a mix of Cas9 protein and short guide RNAs (sgRNAs). This induces clonal regions that are mutant for the target gene throughout the germline and soma. We first injected two sgRNAs targeted for the *white* gene (located on the X chromosome) to calibrate the efficiency of these experiments and

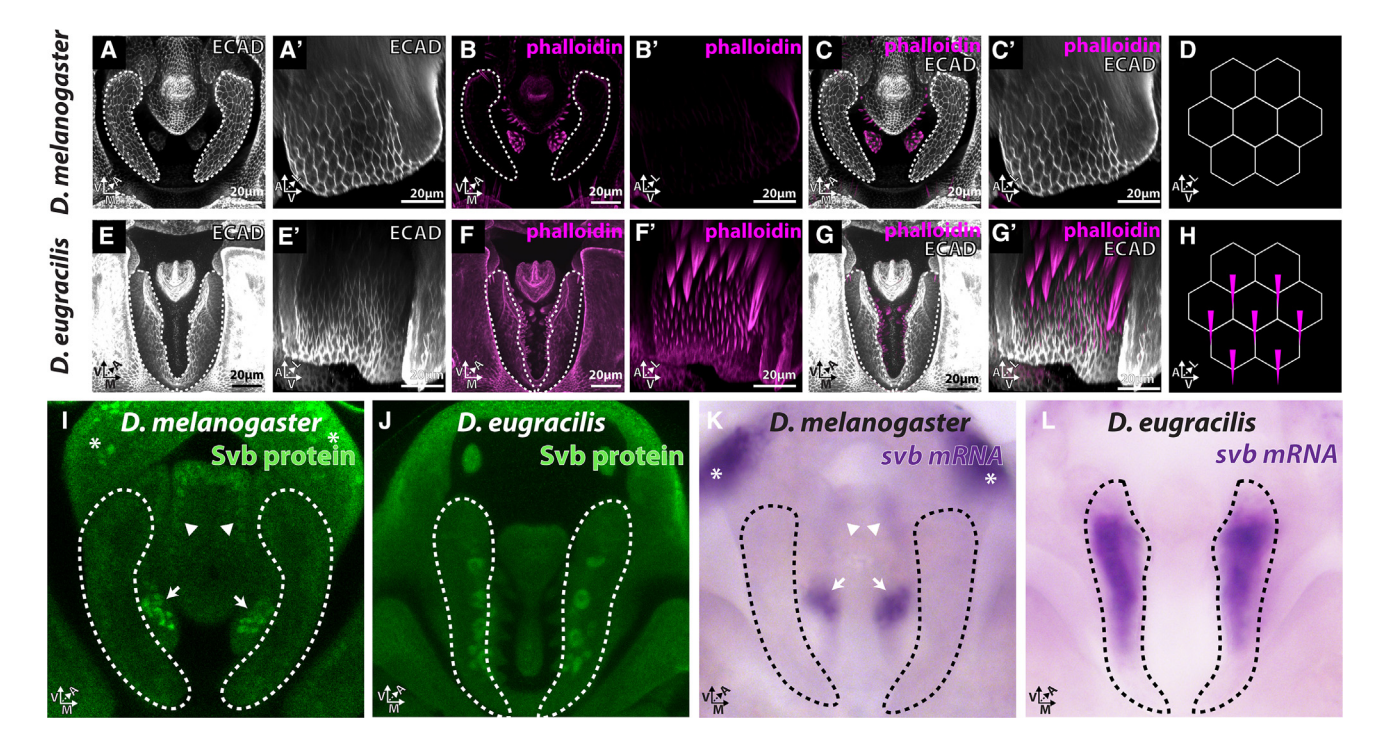


Figure 2. D. eugracilis postgonal sheath projections are unicellular trichomes that express shavenbaby

(A–H) ECAD staining (white) highlights apical cellular junctions, and phalloidin staining (magenta) visualizes actin in the 48 h APF phallus of *D. melanogaster* and *D. eugracilis*. Scale bar, 20 um.

(A–L) Posterior viewpoint. (A'–G') Medial viewpoint.

(A and A') The apical cell junctions of the D. melanogaster postgonal sheath (white dotted lines).

(B and B') Phalloidin staining shows strong concentrations of actin-rich apical projections from the aedeagus and dorsal postgonal processes. See also Figure S3.

(C and C') Composite images show that the D. melanogaster postgonal sheath lacks actin bundles.

(D) A schematic representation depicting the medial cells of the D. melanogaster postgonal sheath.

(E and E') The apical cell junctions of the D. eugracilis postgonal sheath (white dotted lines) show that the postgonal sheath is comprised of a continuous flat plate-shaped structure.

(F and F') Phalloidin staining shows that strong concentrations of actin are present in the *D. eugracilis* postgonal sheath. A time course of phalloidin staining can be found in Figure S2.

(G and G') Composite images show that the postgonal sheath is covered with unicellular actin bundles.

(H) A schematic representation depicting the medial cells of the D. eugracilis postgonal sheath.

(I) Shavenbaby antibody staining of the *D. melanogaster* phallus. Shavenbaby is not highly expressed in the postgonal sheath but is expressed in the aedeagus (arrowheads), medium gonocoxite (asterisks), and dorsal postgonal process (arrows). Shavenbaby antibody staining of the embryo can be found in Figure S4. (J) Shavenbaby antibody staining of the *D. eugracilis* phallus. Shavenbaby is expressed in the medial postgonal sheath as well as the medium gonocoxite. The ventral-anterior *svb* expressing nuclei of the postgonal sheath are large in size.

(K) In situ hybridization for the long isoform of shavenbaby in the D. melanogaster phallus. shavenbaby RNA is not highly expressed in the postgonal sheath but is expressed in the aedeagus (arrowheads), medium gonocoxite (asterisks), and dorsal postgonal process (arrows).

(L) In situ hybridization for shavenbaby in the D. eugracilis phallus. shavenbaby RNA is expressed in the medial postgonal sheath and medium gonocoxite. A time course of shavenbaby in situ hybridization can be found in Figure S2.

produce a negative control, as *white* has no known genital phenotypes. 43.1% of surviving adult males showed a white mosaic patch in the adult eye (Figure S6B; Table S3).

For our svb CRISPR experimental treatment, we used an injection mix that contained Cas9 as well as four sgRNAs (two sgRNAs for white and two sgRNAs for svb). We performed a pilot study where we injected three different combinations of two sgRNAs targeting svb. For most animals, the postgonal sheath trichomes appeared similar to our control injections. However, we noticed that the large trichomes (referred to as major trichomes hereafter) were reduced in size in many of our dissected sheaths (Figure S7A). All three combinations of sgRNAs produced individuals with reduced major trichomes (Figure S8).

Due to a limited number of individuals with mutant phenotypes for each sgRNA combination, we elected to focus on sgRNA pair svb sgRNA 1 and 2 to survey a greater number of injected individuals

For our large-scale *svb* sgRNA 1 and 2 injections (co-injected with *white* sgRNA 3 and 4), 42.7% of our surviving males had mosaic white patches in their eyes, while 16% (9/56) of male adults showed a significant decrease (>3 SD below the *white* control injection mean) in the length of the tallest trichome (Figures 4D, S6B, and S7; Table S3). The lower proportion of identified *svb* major trichome mutants compared with white eye mutants is likely due to us only focusing on two major trichome cells for *svb* mutants, while we detected any white



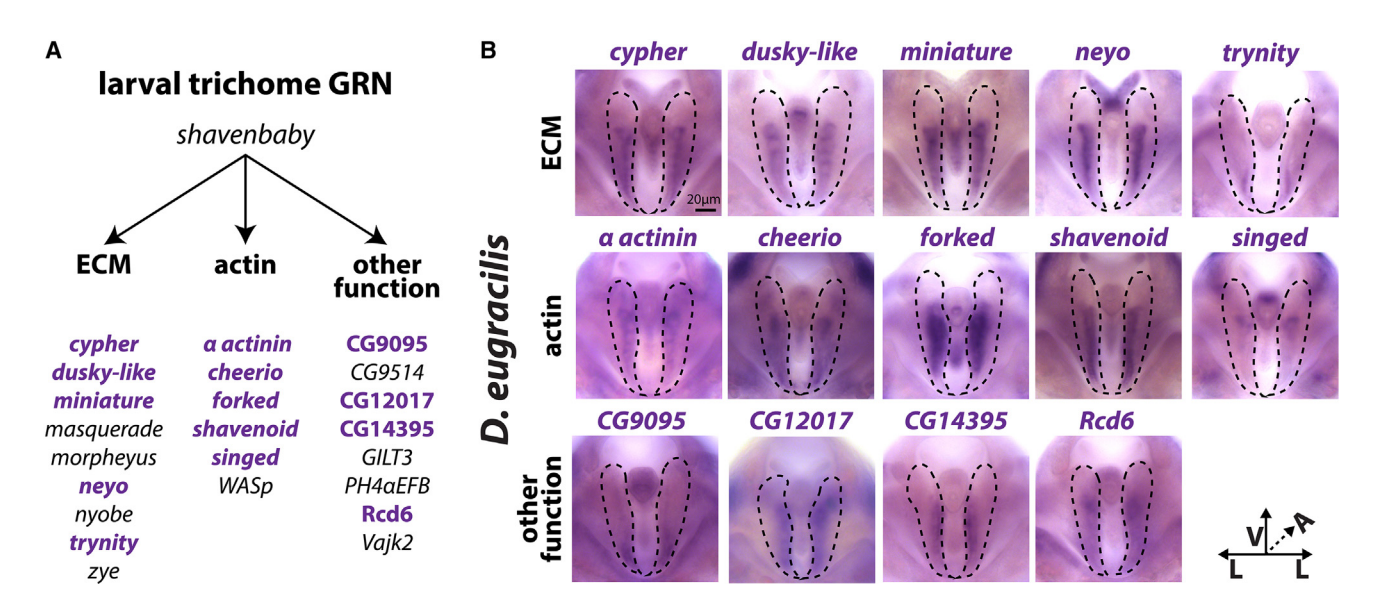


Figure 3. A large portion of the larval trichome GRN is expressed in the D. eugracilis postgonal sheath

(A) Genes within the established larval trichome network that were tested. Bolded purple text indicates the genes expressed in the medial postgonal sheath of *D. eugracilis*; see also Table S1.

(B) In situ hybridization of the *D. eugracilis* 48 h APF developing phallus. Dashed outlines highlight the postgonal sheath. Images of the genes not expressed in the postgonal sheath are found in Figure S5. Each panel is imaged from the posterior perspective, with the ventral side facing up. The expression of each of these genes in the dorsal and ventral larval trichomes can be found in Table S2 and in the medium gonocoxite in Table S5.

patch across the entirety of the eye for *white* mutants. Our results indicate that *svb* is necessary for the wildtype height of the largest postgonal sheath trichomes but that there is likely a redundant system that induces unicellular trichomes in the postgonal sheath independently of *svb*.

The transcription factor *SoxN* is known to partially compensate for *svb* loss for larval trichomes in *svb* null lines, leading to the retention of a reduced number of heavily blunted trichomes.³⁷ To test if *SoxN* may also play a role in the postgonal sheath trichomes of *D. eugracilis*, we performed *in situ* hybridization for *SoxN* in the developing phallus (48 h APF) of *D. melanogaster* and *D. eugracilis*. We observed strong *SoxN* expression in the medial region of the *D. eugracilis* postgonal sheath (similar to *svb* expression) and did not find strong expression in the postgonal sheath of *D. melanogaster* (Figure S2).

svb is sufficient to induce phallic trichomes and a portion of the larval trichome GRN in the postgonal sheath

The expression of the *svb* and several of its downstream genes from the larval trichome genetic network in the postgonal sheath of *D. eugracilis* provides strong evidence for the partial co-option of a core trichome network to the novel context of the *D. eugracilis* postgonal sheath. This suggests that the initial deployment of trichomes in this tissue could have been caused by novel ectopic expression of *svb*. To assess the likelihood of this possibility, we expressed the active form of *svb* using the UAS-*ovoB* line, ³⁵ in the postgonal sheath of *D. melanogaster* (which naturally lacks postgonal trichomes) driven by the phallic *PoxN*-GAL4 driver (PoxN>>ovoB). ^{13,51} Expressing the active form of *svb* was sufficient to induce small trichomes throughout the adult sheath, transforming the *D. melanogaster* postgonal

sheath to a morphology that partially phenocopies the morphology of *D. eugracilis* (Figure 5A).

We next investigated how the induced postgonal sheath trichomes develop in *D. melanogaster*. Co-staining for actin (phalloidin) and apical cell junctions (ECAD) revealed that the induced projections are indeed unicellular (Figure 5B). Although *PoxN*-Gal4 induces expression on the lateral and medial sides of the postgonal sheath, we only observed trichomes forming on the medial side. Additionally, some cells produced multiple trichomes, which was not observed in the *D. eugracilis* postgonal sheath (Figure 5B).

To determine the composition of the GRN of induced phallic trichomes in D. melanogaster, we stained 17 of the downstream members of the larval trichome GRN in these animals. In total, 12 of 17 larval trichome cellular effectors gained expression in the medial postgonal sheath when svb was misexpressed (Table S2). We also found that 4 of our 17 genes showed expression in the medial postgonal sheath of control D. melanogaster, indicating that a portion of the larval trichome genetic network is activated in this naive context (Figure S10). However, two of the 17 genes (neyo and nyobe) show decreased expression patterns in the PoxN>>ovoB background, suggesting that svb or other members of this induced network in D. melanogaster may repress these genes. Conversely, the other two genes (cyr, Vajk2) showed weak localized expression in control D. melanogaster postgonal sheaths and expanded expression in PoxN>>ovoB D. melanogaster, indicating that svb is competent to expand their existing expression. We also found the medium gonocoxite of D. melanogaster (which expresses svb and displays trichomes) expresses 11 out 17 of the larval trichome GRN that we analyzed (Figure S10; Table S5). Our findings provide strong evidence that svb expression is sufficient to induce a

Current Biology Article



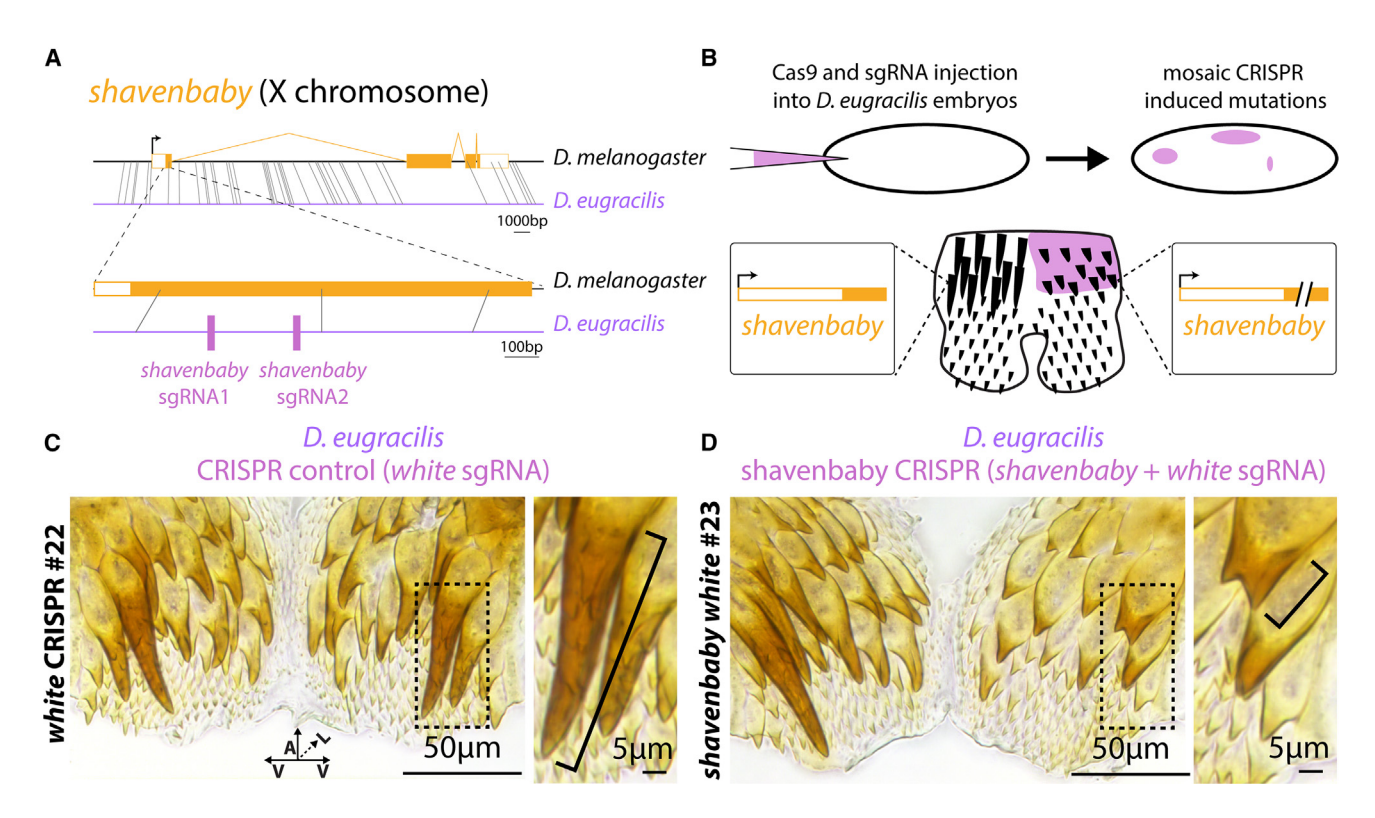


Figure 4. svb is necessary for the postgonal sheath major trichome height

(A) Schematic of the gene shavenbaby (svb). White boxes represent non-coding exons, orange boxes represent coding exons, and lines represent introns. Gray lines represent blocks of homology between D. melanogaster (black line) and D. eugracilis (purple line), with \geq 40 bp perfect identity used for the whole gene view (top) and \geq 30 bp perfect identity used for the zoom-in view (bottom). Target sites for the 2 svb sgRNAs (pink bars). Scale bar, 1,000 bp (top) and 100 bp (bottom). (B) Schematic overview of the CRISPR injection procedure. Cas9 and sgRNAs (pink) are injected into <1-h-old embryos, which will induce mutations in a mosaic pattern. Thus, the adult postgonal sheath of injected individuals will have a subset of cells with mutations (slanted lines on the gene schematic).

(C) A control postgonal sheath (*white* sgRNA + Cas9 injection mix). Representative samples of eye phenotypes are in Figure S6. Dashed box represents the area of the zoom-in (right). Brackets represent the measured height of the largest trichome ("major trichome") on that side. Measurements of major trichome height are found in Table S3. Scale bar, 50 µm (left) and 5 µm (right).

(D) A representative sample of the postgonal sheath when *shavenbaby* was targeted (*white* sgRNA + svb sgRNA + Cas9 injection mix). Additional postgonal sheath samples are found in Figure S7. Dashed box represents the area of the zoom-in (right). Brackets represent the measured height of the largest trichome on that side. Images of representative postgonal sheath samples using different sgRNAs to target *shavenbaby* are found in Figure S8. Sanger sequencing validation of representative samples is found in Figure S9. Scale bar, 50 μm (left) and 5 μm (right).

large portion of the larval trichome GRN in the $\it{D.}$ melanogaster postgonal sheath.

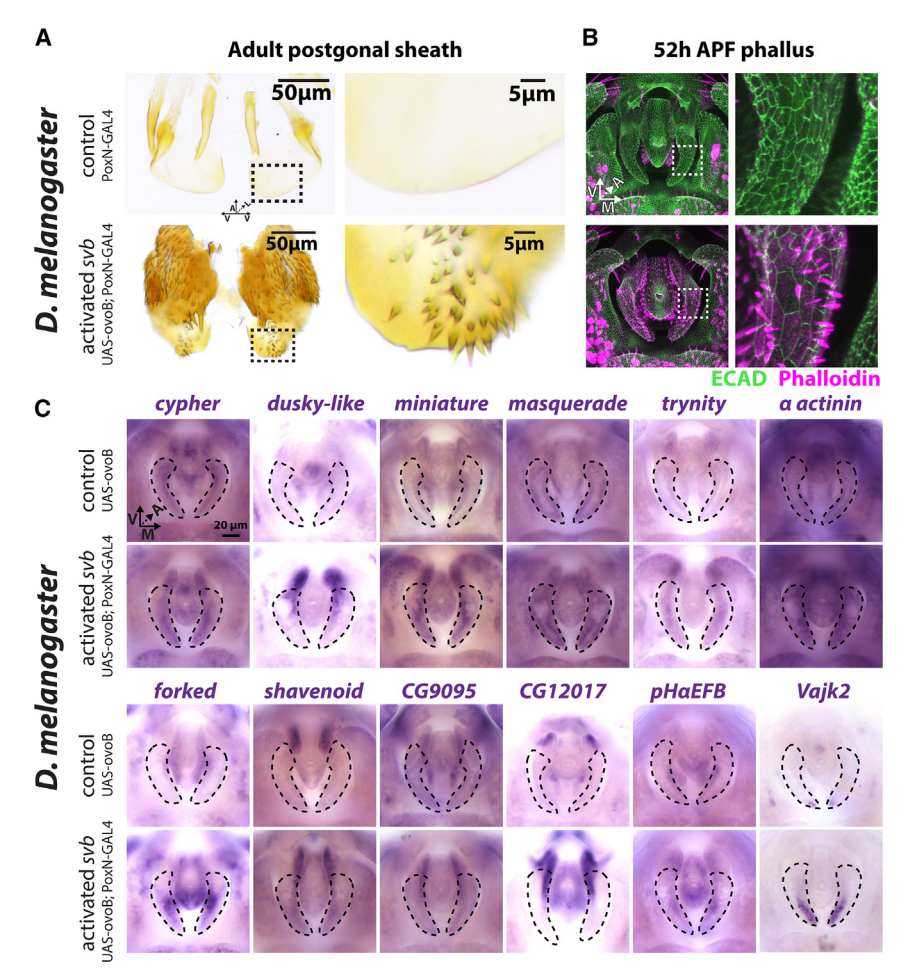
DISCUSSION

The origins of morphological novelty have long fascinated evolutionary biologists with the conundrum of how a completely new structure might first arise and subsequently adopt its elaborate morphology. Our findings provide evidence that the novel postgonal sheath projections of *D. eugracilis* were generated through the partial co-option and subsequent modification of an ancestral trichome genetic network. The examination of known larval trichome genetic network genes identified a core subset of 14 genes shared between larval and postgonal sheath trichomes, including the key transcription factor-encoding genes *svb* and *SoxN*. Loss-of-function studies demonstrate how *svb* is required for sheath trichome morphology in *D. eugracilis*, consistent with the co-option of this network. Moreover, the induction of small trichomes by *svb* misexpression in *D. melanogaster* illustrates how these trichomes may have first appeared in the

D. eugracilis lineage and highlight the extreme modifications that some of these trichomes underwent as the structures became more specialized. The rewiring of this network that led to this specialized size and shape best encapsulates what makes these trichomes novel rather than a mere repetition of trichome morphologies seen in other parts of the body (Figure 6).

The *D. eugracilis* postgonal sheath trichomes appear to be a novelty as they do not appear in other members of the *melanogaster*, *suzukii*, *ananassae*, and *pseudoobscura* subgroups we have previously investigated via microdissection of the adult genitalia. ²⁴ Bock and Wheeler previously characterized the overall genital morphology of the *melanogaster* species groups. ²³ In their analysis, the phallus of *D. elegans* (*suzukii* subgroup), and *D. ficusphila* (*ficusphila* species group), and *D. orosa* (*montium* species group) have what appear to be bumps near the area of the postgonal sheath. Further characterization of the adult morphology, development, and *svb* expression patterns of these species will be needed to establish if these bumps are trichomes and if there is a deeper origin of the postgonal sheath trichomes.





focused on larval trichomes. 35,37-39 but trichomes are found across the adult body plan in various shapes and sizes, from the sawtooth-shaped trichomes of the female genitalia to the long, thin trichomes that comprise the arista of the antenna. 31,35,46 The adult leg trichome genetic network was found to be rewired, 12 with 83% (135/163) of the genes known to be bound by svb expressed above background levels in the developing leg transcriptome. This suggests that changes exist in the enhancers and trans environments between these two distinct developmental contexts. The medium gonocoxite trichomes of both D. eugracilis (Figure S5) and D. melanogaster (Figure S10) express only a subset (\sim 50%) of the tested larval trichome GRN genes (Table S5). Even the trichomes of the larvae differ in the expression of downstream targets of svb, with 91% and 96% of the genes we analyzed being expressed in the dorsal and ventral trichomes, respectively. The variation in the percentage of the genetic network expressed across trichome type and developmental stages leads us to expect that the co-option of the trichome genetic network will be partial and not wholescale²⁰ in nature even during its initiation.

The majority of the research on the svb genetic network has

Indeed, we observe that 71% of the 17 tested larval trichome genes are active when *svb* is ectopically expressed in the *D. melanogaster* postgonal sheath.²⁰ The percentage of larval trichome genes drops to 60% in the postgonal sheath of

Figure 5. Activated *svb* is sufficient to induce trichomes and a portion of the larval trichome GRN in *D. melanogaster*

(A) Top: the control adult postgonal sheath (UAS-ovoB) has a smooth morphology. Bottom: induction of the activated form of *shavenbaby* (PoxN-GAL4; UAS-ovoB) in the adult postgonal sheath generates small trichomes. Dotted boxes show the closeup view region to the right. Scale bar, 50 μ m (left) and 5 μ m (right).

(B) The developing phallus of the control and *shavenbaby*-induced samples stained with ECAD (green) and phalloidin (magenta). Controls (top) do not produce any unicellular actin outgrowth while *shavenbaby*-induced (PoxN-GAL4; UAS-ovoB) samples gain unicellular actin bundles. There is variation in the induced trichomes, with some cells producing multiple actin projections while others produce one or no actin projections.

(C) In situ hybridization for 12 downstream targets of the larval trichome genetic network in control and active shavenbaby 48 h APF developing phalluses; see also Figure S10 and Table S1. Expression of these genes in the medium gonocoxite can be found in Figure S10 and Table S5.

D. eugracilis, indicating that the genetic network in the postgonal sheath may have specialized after it first evolved, allowing these trichomes to gain their unique characteristics. Even the trichomes within the *D. eugracilis* postgonal sheath vary in size, with the major trichomes possessing enlarged nuclei that could be established via endoreplication, i.e., localized polyploidy.⁵² Large trichome-like structures

have been found in the larvae of botflies and have been suggested as a means to prevent their extraction. ^{53,54} This mechanism could explain how a unicellular outgrowth rivals the size of novel multicellular outgrowths like the dorsal and ventral postgonal processes found in *D. melanogaster*. ²⁴ That two distinct cellular mechanisms (unicellular and multicellular) are responsible for similarly sized and shaped novelties (Figure 1) provides a clear example of phenotypic convergence. Studying which genes are necessary for different trichome types will allow us to distinguish between the core trichome genetic network and genes that are non-essential but modify cell shape in specific contexts

In *Drosophila melanogaster* larvae, *svb* mutants lose most of the ventral trichomes and many of the dorsal trichomes. The ventral and dorsal trichomes that remain in *svb* mutants have reduced height, ^{33,37} which is similar to what we observe in CRISPR-induced *svb* knockout clones in the postgonal sheath of *D. eugracilis*. This reduction of height is also seen in the trichomes of the wing, leg, and abdomen in *svb* mutants. ³⁴ The incomplete loss of larval trichomes is thought to be due to the potential redundancy of the transcription factor *SoxN*, which is sufficient to induce larval trichomes independent of *svb*. ³⁷ We found that *SoxN* is expressed in the postgonal sheath of *D. eugracilis*, suggesting that it may be necessary to disrupt both genes to induce a loss of postgonal sheath trichomes.

Current Biology





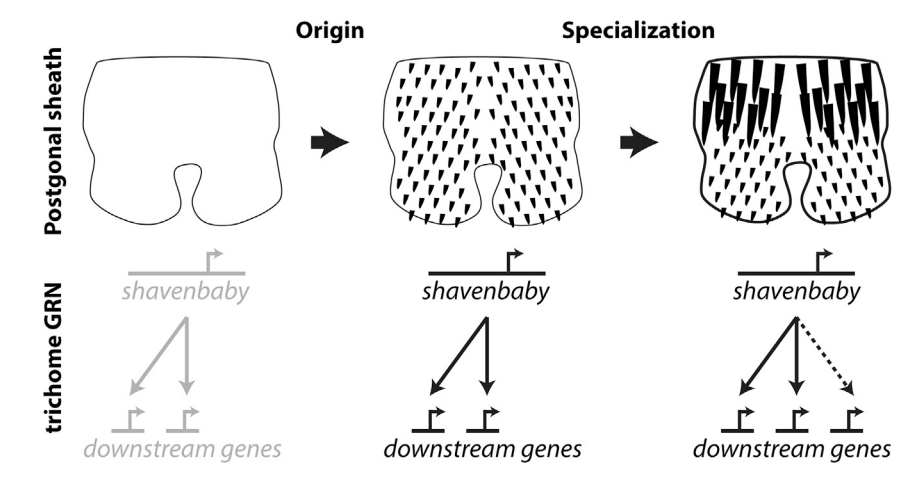


Figure 6. Model of the origin and specialization of the D. eugracilis postgonal sheath tri-

The postgonal sheath of D. melanogaster lacks trichomes and the expression of the larval trichome genetic network. The expression of svb in D. melanogaster (black arrow) induces small postgonal trichomes and much of the larval trichome genetic network. We find that some members of the larval trichome network are expressed in D. eugracilis, which naturally houses postgonal trichomes, and not when svb is expressed in D. melanogaster (dashed line), indicating that the postgonal sheath trichome network may have evolved to incorporate these genes. We predict that specialization (black arrow) allowed D. eugracilis to exhibit a unique genetic network leading to a diversity of trichome sizes.

The redundancy of this network begs the question of what genetic changes were sufficient to first establish this novel trichome tvpe.

The theory of the GRN co-option suggests that novel traits can be initiated through the activation of top-tier members of a genetic network in a tissue that did not previously express that genetic network. This would potentially allow hundreds of genes to gain and lose expression in that formerly naive tissue, inducing a large morphological shift. This theory has been implicated in the origin of the beetle horn, 16 echinoderm embryonic skeletons, 55 treehopper helmets, 17 and many more. 56 However, to our knowledge, only a single other study has shown that a morphological novelty can be induced through the ectopic expression of an upstream gene. 18 Marcellini and Simpson 18 showed that Drosophila quadrilineata possesses an increased number of dorsocentral bristles (four pairs) in their thorax compared with D. melanogaster (two pairs). The authors further showed that the D. quadrilineata enhancer of the proneural scute gene was sufficient to induce the two extra pairs of bristles when driving scute expression in D. melanogaster. The D. quadralineata study shows the ability of a genetic network co-option to induce additional copies of the same trait. On the other hand, the unique size and shape of the D. eugracilis postgonal sheath trichomes represents a system where one can test how repeated traits evolve unique features independent of the structure from which it was co-opted.

Although a core GRN may be shared between the co-opted and novel traits, some genes in the bottom tier of the network may become specific to each context and impart specialized characteristics. 1,20,57,58 This can be seen in novelties such as the tusk of a narwhal. The tusk has been found to be a modified canine tooth, yet this structure is unique in its size and straight spiral shape when compared with other toothed whales, odontocetes, as well as its remaining vestigial teeth.⁵⁹ One could make the case that the tusk is not a true novelty, as it is clearly recognized as a modified tooth. Yet it is the unusual characteristics, not the presence of a clear homology, that pull our focus to these specific structures. If the tusk was simply another tooth with the same repeated morphology in a new position of the body plan, it may not have garnered the same interest or fascination. Future work focusing on how genetic networks add, remove, and modify genes to evolve a specialized morphology in new contexts of the body plan will provide a much-needed perspective of what makes a trait novel.

RESOURCE AVAILABILITY

Lead contact

Further information and requests for resources and reagents should be directed to and will be fulfilled by the lead contact, Mark Rebeiz (rebeiz@pitt.

Materials availability

This study did not generate new unique reagents.

Data and code availability

- Original data underlying this manuscript can be accessed from the Stowers Original Data Repository at https://www.stowers.org/research/ publications/libpb-2489 and are publicly available as of the date of publication. Links are listed in the key resources table.
- This paper does not report original code
- Any additional information required to reanalyze the data reported in this paper is available from the lead contact upon request.

ACKNOWLEDGMENTS

We would like to thank David Stern Ella Preger-Ben-Noon, Nicolas Frankel, Priscilla Erickson, Michelle Pogrebetskaya, Haley Salus, Kathryn Ono, and Priyadarshini for their comments on this manuscript and project; Cindi Staber and the Zeitlinger lab for designing the shavenbaby antibody; and Dai Tsuchiya and Nancy Thomas for assistance in the histology of shavenbaby in the embryo. Thanks to the lab of Kate O'Connor-Giles for adding D. eugracilis to the CRISPR Optimal Target Finder website. We thank the entire Rebeiz lab, Ben Vincent, Omid Saleh Ziabari, Yang Liu, Sarah Smith, Eden McQueen, Donya Shodja, Iván Méndez-González, Sarah Petrosky, Catarina Colmatti Bromatti, Casey Guidry, and Chris Darfoor, for support and providing comments on the manuscript. Funding was provided by the National Institutes of Health (R21HD104956 to M.R. and K99GM147343-01 to G.R.) and by the Stowers Institute for Medical Research through J.Z.

AUTHOR CONTRIBUTIONS

The project was conceived by G.R. and M.R. Experiments were carried out by G.R., T.G.-E., and K.C.-O. Data were analyzed by all authors. G.R. and M.R. wrote the paper, assisted by J.Z., T.G.-E., and K.C.-O.





DECLARATION OF INTERESTS

The authors declare no competing interests.

STAR*METHODS

Detailed methods are provided in the online version of this paper and include the following:

- KEY RESOURCES TABLE
- EXPERIMENTAL MODEL AND STUDY PARTICIPANT DETAILS
 - Drosophila strains
- METHOD DETAILS
 - o Sample collection, dissection, and fixation
 - o Probe design and synthesis
 - Antibody generation
 - o CRISPR
 - Imaging
- QUANTIFICATION AND STATISTICAL ANALYSIS

SUPPLEMENTAL INFORMATION

Supplemental information can be found online at https://doi.org/10.1016/j.cub.2024.09.073.

Received: March 30, 2024 Revised: July 25, 2024

Accepted: September 25, 2024 Published: October 25, 2024

REFERENCES

- Hu, Y., Schmitt-Engel, C., Schwirz, J., Stroehlein, N., Richter, T., Majumdar, U., and Bucher, G. (2018). A morphological novelty evolved by co-option of a reduced gene regulatory network and gene recruitment in a beetle. Proc. Biol. Sci. 285, 20181373. https://doi.org/10.1098/rspb. 2018.1373
- Monteiro, A. (2012). Gene regulatory networks reused to build novel traits: co-option of an eye-related gene regulatory network in eye-like organs and red wing patches on insect wings is suggested by optix expression. BioEssays 34, 181–186. https://doi.org/10.1002/bies.201100160.
- True, J.R., and Carroll, S.B. (2002). Gene co-option in physiological and morphological evolution. Annu. Rev. Cell Dev. Biol. 18, 53–80. https://doi.org/10.1146/annurev.cellbio.18.020402.140619.
- Hatleberg, W.L., and Hinman, V.F. (2021). Chapter Two Modularity and hierarchy in biological systems: Using gene regulatory networks to understand evolutionary change. In Current Topics in Developmental Biology Evolutionary Developmental Biology, S.F. Gilbert, ed. (Academic Press), pp. 39–73. https://doi.org/10.1016/bs.ctdb.2020.11.004.
- Stern, P.D. (2010). Evolution, Development, and the Predictable Genome, First Edition (Roberts and Company Publishers).
- Stern, D.L., and Orgogozo, V. (2008). The loci of evolution: how predictable is genetic evolution? Evolution 62, 2155–2177. https://doi.org/10.1111/j. 1558-5646.2008.00450.x.
- Barkoulas, M., Hay, A., Kougioumoutzi, E., and Tsiantis, M. (2008). A developmental framework for dissected leaf formation in the Arabidopsis relative Cardamine hirsuta. Nat. Genet. 40, 1136–1141. https://doi.org/10.1038/ng.189.
- Fraser, G.J., Hulsey, C.D., Bloomquist, R.F., Uyesugi, K., Manley, N.R., and Streelman, J.T. (2009). An ancient gene network is co-opted for teeth on old and new jaws. PLoS Biol. 7, e31. https://doi.org/10.1371/journal. pbio.1000031.
- Knox, K., and Baker, J.C. (2008). Genomic evolution of the placenta using co-option and duplication and divergence. Genome Res. 18, 695–705. https://doi.org/10.1101/gr.071407.107.

- Moczek, A.P., and Nagy, L.M. (2005). Diverse developmental mechanisms contribute to different levels of diversity in horned beetles. Evol. Dev. 7, 175–185. https://doi.org/10.1111/j.1525-142X.2005.05020.x.
- Moczek, A.P., and Rose, D.J. (2009). Differential recruitment of limb patterning genes during development and diversification of beetle horns. Proc. Natl. Acad. Sci. USA 106, 8992–8997. https://doi.org/10.1073/ pnas.0809668106.
- Kittelmann, S., Buffry, A.D., Franke, F.A., Almudi, I., Yoth, M., Sabaris, G., Couso, J.P., Nunes, M.D.S., Frankel, N., Gómez-Skarmeta, J.L., et al. (2018). Gene regulatory network architecture in different developmental contexts influences the genetic basis of morphological evolution. PLoS Genet. 14, e1007375. https://doi.org/10.1371/journal.pgen.1007375.
- Glassford, W.J., Johnson, W.C., Dall, N.R., Smith, S.J., Liu, Y., Boll, W., Noll, M., and Rebeiz, M. (2015). Co-option of an ancestral Hox-regulated network underlies a recently evolved morphological novelty. Dev. Cell 34, 520–531. https://doi.org/10.1016/j.devcel.2015.08.005.
- Molina-Gil, S., Sotillos, S., Espinosa-Vázquez, J.M., Almudi, I., and Hombría, J.C.-G. (2023). Interlocking of co-opted developmental gene networks in Drosophila and the evolution of pre-adaptive novelty. Nat. Commun. 14, 5730. https://doi.org/10.1038/s41467-023-41414-3.
- Martin, A., McCulloch, K.J., Patel, N.H., Briscoe, A.D., Gilbert, L.E., and Reed, R.D. (2014). Multiple recent co-options of Optix associated with novel traits in adaptive butterfly wing radiations. EvoDevo 5, 7. https:// doi.org/10.1186/2041-9139-5-7.
- Hu, Y., Linz, D.M., and Moczek, A.P. (2019). Beetle horns evolved from wing serial homologs. Science 366, 1004–1007. https://doi.org/10.1126/ science.aaw2980.
- Fisher, C.R., Wegrzyn, J.L., and Jockusch, E.L. (2020). Co-option of wingpatterning genes underlies the evolution of the treehopper helmet. Nat. Ecol. Evol. 4, 250–260. https://doi.org/10.1038/s41559-019-1054-4.
- Marcellini, S., and Simpson, P. (2006). Two or four bristles: functional evolution of an enhancer of scute in Drosophilidae. PLoS Biol. 4, e386. https:// doi.org/10.1371/journal.pbio.0040386.
- Zeitlinger, J., and Bohmann, D. (1999). Thorax closure in Drosophila: involvement of Fos and the JNK pathway. Development 126, 3947–3956. https://doi.org/10.1242/dev.126.17.3947.
- McQueen, E., and Rebeiz, M. (2020). On the specificity of gene regulatory networks: How does network co-option affect subsequent evolution? Curr. Top. Dev. Biol. 139, 375–405. https://doi.org/10.1016/bs.ctdb. 2020.03.002.
- Hsu, T. (1949). The external genital apparatus of male Drosophilidae in relation to systematics. Univ. Tex. Publ. 4920, 80–142.
- Okada, T. (1954). Comparative morphology of the drosophilid flies. I. Phallic organs of the melanogaster group. Kontyu 22, 36–46.
- Bock, I., and Wheeler, M. (1972). The Drosophila melanogaster species group, Univ. Tex. Publ. 7, 1–102.
- Rice, G.R., David, J.R., Gompel, N., Yassin, A., and Rebeiz, M. (2023).
 Resolving between novelty and homology in the rapidly evolving phallus of Drosophila. J. Exp. Zool. B Mol. Dev. Evol. 340, 182–196. https://doi.org/10.1002/jez.b.23113.
- Finet, C., Kassner, V.A., Carvalho, A.B., Chung, H., Day, J.P., Day, S., Delaney, E.K., De Ré, F.C., Dufour, H.D., Dupim, E., et al. (2021). DrosoPhyla: resources for Drosophilid phylogeny and systematics. Genome Biol. Evol. 13, evab179. https://doi.org/10.1093/gbe/evab179.
- Wong, A., Jensen, J.D., Pool, J.E., and Aquadro, C.F. (2007). Phylogenetic incongruence in the Drosophila melanogaster species group. Mol. Phylogenet. Evol. 43, 1138–1150. https://doi.org/10.1016/j.ympev.2006.09.002
- Ko, W.-Y., David, R.M., and Akashi, H. (2003). Molecular phylogeny of the Drosophila melanogaster species subgroup. J. Mol. Evol. 57, 562–573. https://doi.org/10.1007/s00239-003-2510-x.
- Rice, G., David, J.R., Kamimura, Y., Masly, J.P., Mcgregor, A.P., Nagy, O., Noselli, S., Nunes, M.D.S., O'Grady, P., Sánchez-Herrero, E., et al. (2019).
 A standardized nomenclature and atlas of the male terminalia of

Current Biology

Article



- Drosophila melanogaster. Fly (Austin) 13, 51–64. https://doi.org/10.1080/19336934.2019.1653733.
- Kamimura, Y. (2010). Copulation anatomy of Drosophila melanogaster (Diptera: Drosophilidae): wound-making organs and their possible roles. Zoomorphology 129, 163–174. https://doi.org/10.1007/s00435-010-0109-5.
- Stern, D.L., and Frankel, N. (2013). The structure and evolution of cis-regulatory regions: the shavenbaby story. Philos. Trans. R. Soc. Lond. B Biol. Sci. 368, 20130028. https://doi.org/10.1098/rstb.2013.0028.
- Arif, S., Kittelmann, S., and McGregor, A.P. (2015). From shavenbaby to the naked valley: trichome formation as a model for evolutionary developmental biology. Evol. Dev. 17, 120–126. https://doi.org/10.1111/ede. 12113
- Delon, I., and Payre, F. (2004). Evolution of larval morphology in flies: get in shape with shavenbaby. Trends Genet. 20, 305–313. https://doi.org/10. 1016/i.tig.2004.05.003.
- Payre, F., Vincent, A., and Carreno, S. (1999). ovo/svb integrates Wingless and DER pathways to control epidermis differentiation. Nature 400, 271–275. https://doi.org/10.1038/22330.
- Preger-Ben Noon, E., Sabarís, G., Ortiz, D.M., Sager, J., Liebowitz, A., Stern, D.L., and Frankel, N. (2018). Comprehensive analysis of a cis-regulatory region reveals pleiotropy in enhancer function. Cell Rep. 22, 3021–3031. https://doi.org/10.1016/j.celrep.2018.02.073.
- Delon, I., Chanut-Delalande, H., and Payre, F. (2003). The Ovo/ Shavenbaby transcription factor specifies actin remodelling during epidermal differentiation in Drosophila. Mech. Dev. 120, 747–758. https://doi.org/10.1016/S0925-4773(03)00081-9.
- Sucena, E., and Stern, D.L. (2000). Divergence of larval morphology between Drosophila sechellia and its sibling species caused by cis-regulatory evolution of ovo/shaven-baby. Proc. Natl. Acad. Sci. USA 97, 4530–4534. https://doi.org/10.1073/pnas.97.9.4530.
- Rizzo, N.P., and Bejsovec, A. (2017). SoxNeuro and shavenbaby act cooperatively to shape denticles in the embryonic epidermis of Drosophila. Development 144, 2248–2258. https://doi.org/10.1242/dev.150169.
- Menoret, D., Santolini, M., Fernandes, I., Spokony, R., Zanet, J., Gonzalez, I., Latapie, Y., Ferrer, P., Rouault, H., White, K.P., et al. (2013). Genome-wide analyses of Shavenbaby target genes reveals distinct features of enhancer organization. Genome Biol. 14, R86. https://doi.org/10.1186/gb-2013-14-8-r86.
- Chanut-Delalande, H., Fernandes, I., Roch, F., Payre, F., and Plaza, S. (2006). Shavenbaby couples patterning to epidermal cell shape control. PLoS Biol. 4, e290. https://doi.org/10.1371/journal.pbio.0040290.
- Sucena, E., Delon, I., Jones, I., Payre, F., and Stern, D.L. (2003). Regulatory evolution of shavenbaby/ovo underlies multiple cases of morphological parallelism. Nature 424, 935–938. https://doi.org/10. 1038/nature01768.
- McGregor, A.P., Orgogozo, V., Delon, I., Zanet, J., Srinivasan, D.G., Payre, F., and Stern, D.L. (2007). Morphological evolution through multiple cisregulatory mutations at a single gene. Nature 448, 587–590. https://doi. org/10.1038/nature05988.
- Frankel, N., Davis, G.K., Vargas, D., Wang, S., Payre, F., and Stern, D.L. (2010). Phenotypic robustness conferred by apparently redundant transcriptional enhancers. Nature 466, 490–493. https://doi.org/10.1038/nature09158
- Soverna, A.F., Rodriguez, N.C., Korgaonkar, A., Hasson, E., Stern, D.L., and Frankel, N. (2021). Cis-regulatory variation in the shavenbaby gene underlies intraspecific phenotypic variation, mirroring interspecific divergence in the same trait. Evolution 75, 427–436. https://doi.org/10.1111/ evo.14142.
- Payre, F. (2004). Genetic control of epidermis differentiation in Drosophila.
 Int. J. Dev. Biol. 48, 207–215. https://doi.org/10.1387/ijdb.15272387.
- McQueen, E.W., Afkhami, M., Atallah, J., Belote, J.M., Gompel, N., Heifetz, Y., Kamimura, Y., Kornhauser, S.C., Masly, J.P., O'Grady, P., et al. (2022). A standardized nomenclature and atlas of the female

- terminalia of Drosophila melanogaster. Fly (Austin) *16*, 128–151. https://doi.org/10.1080/19336934.2022.2058309.
- Tanaka, K.M., Takahashi, K., Rice, G., Rebeiz, M., Kamimura, Y., and Takahashi, A. (2022). Trichomes on female reproductive tract: rapid diversification and underlying gene regulatory network in Drosophila suzukii and its related species. BMC Ecol. Evol. 22, 93. https://doi.org/10.1186/ s12862-022-02046-1.
- Poodry, C.A. (1980). Epidermis: morphology and development. In The Genetics and Biology of Drosophila (Academic Press), pp. 443–497.
- Sabarís, G., Ortíz, D.M., Laiker, I., Mayansky, I., Naik, S., Cavalli, G., Stern, D.L., Preger-Ben Noon, E., and Frankel, N. (2024). The density of regulatory information is a major determinant of evolutionary constraint on noncoding DNA in Drosophila. Mol. Biol. Evol. 41, msae004. https://doi.org/ 10.1093/molbev/msae004.
- Fernandes, I., Chanut-Delalande, H., Ferrer, P., Latapie, Y., Waltzer, L., Affolter, M., Payre, F., and Plaza, S. (2010). Zona pellucida domain proteins remodel the apical compartment for localized cell shape changes. Dev. Cell 18, 64–76. https://doi.org/10.1016/j.devcel.2009.11.009.
- Zhang, L., and Reed, R.D. (2017). A practical guide to CRISPR/Cas9 genome editing in Lepidoptera. In Diversity and Evolution of Butterfly Wing Patterns: An Integrative Approach, T. Sekimura, and H.F. Nijhout, eds. (Springer), pp. 155–172. https://doi.org/10.1007/978-981-10-4956-9 8.
- Boll, W., and Noll, M. (2002). The Drosophila Pox neuro gene: control of male courtship behavior and fertility as revealed by a complete dissection of all enhancers. Development 129, 5667–5681. https://doi.org/10.1242/ dev.00157
- Orr-Weaver, T.L. (2015). When bigger is better: the role of polyploidy in organogenesis. Trends Genet. 31, 307–315. https://doi.org/10.1016/j.tig. 2015.03.011
- Cornet, M., Florent, M., Lefebvre, A., Wertheimer, C., Perez-Eid, C., Bangs, M.J., and Bouvet, A. (2003). Tracheopulmonary myiasis caused by a mature third-instar cuterebra larva: case report and review. J. Clin. Microbiol. 41, 5810–5812. https://doi.org/10.1128/JCM.41.12.5810-5812.2003.
- Shenouda, M., Enten, G., Nguyen, T., Mangar, D., and Camporesi, E. (2018). Human botfly: a case report and overview of differential diagnosis.
 J. Investig. Med. High Impact Case Rep. 6, 2324709618801692. https://doi.org/10.1177/2324709618801692.
- Gao, F., and Davidson, E.H. (2008). Transfer of a large gene regulatory apparatus to a new developmental address in echinoid evolution. Proc. Natl. Acad. Sci. USA 105, 6091–6096. https://doi.org/10.1073/pnas. 0801201105.
- Rebeiz, M., and Tsiantis, M. (2017). Enhancer evolution and the origins of morphological novelty. Curr. Opin. Genet. Dev. 45, 115–123. https://doi. org/10.1016/j.gde.2017.04.006.
- Scheffer, D.I., Shen, J., Corey, D.P., and Chen, Z.-Y. (2015). Gene expression by mouse inner ear hair cells during development. J. Neurosci. 35, 6366–6380. https://doi.org/10.1523/JNEUROSCI.5126-14.2015.
- Chessum, L., Matern, M.S., Kelly, M.C., Johnson, S.L., Ogawa, Y., Milon, B., McMurray, M., Driver, E.C., Parker, A., Song, Y., et al. (2018). Helios is a key transcriptional regulator of outer hair cell maturation. Nature 563, 696–700. https://doi.org/10.1038/s41586-018-0728-4.
- Nweeia, M.T., Eichmiller, F.C., Hauschka, P.V., Tyler, E., Mead, J.G., Potter, C.W., Angnatsiak, D.P., Richard, P.R., Orr, J.R., and Black, S.R. (2012). Vestigial Tooth anatomy and tusk nomenclature for monodon monoceros. Anat. Rec. (Hoboken) 295, 1006–1016. https://doi.org/10. 1002/ar.22449.
- Nassar, L.R., Barber, G.P., Benet-Pagès, A., Casper, J., Clawson, H., Diekhans, M., Fischer, C., Gonzalez, J.N., Hinrichs, A.S., Lee, B.T., et al. (2023). The UCSC Genome Browser database: 2023 update. Nucleic Acids Res. 51, D1188–D1195. https://doi.org/10.1093/nar/gkac1072.
- 61. Untergasser, A., Nijveen, H., Rao, X., Bisseling, T., Geurts, R., and Leunissen, J.A.M. (2007). Primer3Plus, an enhanced web interface to





- Primer3. Nucleic Acids Res. 35, W71–W74. https://doi.org/10.1093/nar/gkm306.
- 62. Gratz, S.J., Ukken, F.P., Rubinstein, C.D., Thiede, G., Donohue, L.K., Cummings, A.M., and O'Connor-Giles, K.M. (2014). Highly specific and efficient CRISPR/Cas9-catalyzed homology-directed repair in Drosophila. Genetics 196, 961–971. https://doi.org/10.1534/genetics. 113.160713.
- Méndez-González, I.D., Williams, T.M., and Rebeiz, M. (2023). Changes in locus wide repression underlie the evolution of Drosophila abdominal pigmentation. PLoS Genet. 19, e1010722. https://doi.org/10.1371/journal.pgen.1010722.
- 64. Barbier de Reuille, P., Routier-Kierzkowska, A.-L., Kierzkowski, D., Bassel, G.W., Schüpbach, T., Tauriello, G., Bajpai, N., Strauss, S., Weber, A., Kiss, A., et al. (2015). MorphoGraphX: A platform for quantifying morphogenesis in 4D. eLife 4, 05864. https://doi.org/10.7554/eLife.05864.
- 65. Vincent, B.J., Rice, G.R., Wong, G.M., Glassford, W.J., Downs, K.I., Shastay, J.L., Charles-Obi, K., Natarajan, M., Gogol, M., Zeitlinger, J., et al. (2019). An atlas of transcription factors expressed in male pupal terminalia of Drosophila melanogaster. G3 (Bethesda) 9, 3961–3972. https://doi.org/10.1534/g3.119.400788.

Current Biology Article



STAR***METHODS**

KEY RESOURCES TABLE

Cat# DCAD2; RRID: AB_528120 N/A Cat# R415 Cat# 15710 BP227500 EMD Millipore Corporation BP1115-500 Cat# F-548L 50-591-966 Cat# 17109821 H8773 H4784 BP337-500 BP151-500 Cat# M0314S Cat# 638909 Cat# 28706 Cat# 69504 Cat# P2075
N/A Cat# R415 Cat# 15710 BP227500 EMD Millipore Corporation BP1115-500 Cat# F-548L 50-591-966 Cat# 17109821 H8773 H4784 BP337-500 BP151-500 Cat# M0314S Cat# 638909 Cat# 28706 Cat# 69504
N/A Cat# R415 Cat# 15710 BP227500 EMD Millipore Corporation BP1115-500 Cat# F-548L 50-591-966 Cat# 17109821 H8773 H4784 BP337-500 BP151-500 Cat# M0314S Cat# 638909 Cat# 28706 Cat# 69504
Cat# R415 Cat# 15710 BP227500 EMD Millipore Corporation BP1115-500 Cat# F-548L 50-591-966 Cat# 17109821 H8773 H4784 BP337-500 BP151-500 Cat# M0314S Cat# 638909 Cat# 28706 Cat# 69504
Cat# 15710 BP227500 EMD Millipore Corporation BP1115-500 Cat# F-548L 50-591-966 Cat# 17109821 H8773 H4784 BP337-500 BP151-500 Cat# M0314S Cat# 638909 Cat# 28706 Cat# 69504
BP227500 EMD Millipore Corporation BP1115-500 Cat# F-548L 50-591-966 Cat# 17109821 H8773 H4784 BP337-500 BP151-500 Cat# M0314S Cat# 638909 Cat# 28706 Cat# 69504
BP227500 EMD Millipore Corporation BP1115-500 Cat# F-548L 50-591-966 Cat# 17109821 H8773 H4784 BP337-500 BP151-500 Cat# M0314S Cat# 638909 Cat# 28706 Cat# 69504
EMD Millipore Corporation BP1115-500 Cat# F-548L 50-591-966 Cat# 17109821 H8773 H4784 BP337-500 BP151-500 Cat# M0314S Cat# 638909 Cat# 28706 Cat# 69504
BP1115-500 Cat# F-548L 50-591-966 Cat# 17109821 H8773 H4784 BP337-500 BP151-500 Cat# M0314S Cat# 638909 Cat# 28706 Cat# 69504
Cat# F-548L 50-591-966 Cat# 17109821 H8773 H4784 BP337-500 BP151-500 Cat# M0314S Cat# 638909 Cat# 28706 Cat# 69504
50-591-966 Cat# 17109821 H8773 H4784 BP337-500 BP151-500 Cat# M0314S Cat# 638909 Cat# 28706 Cat# 69504
Cat# 17109821 H8773 H4784 BP337-500 BP151-500 Cat# M0314S Cat# 638909 Cat# 28706 Cat# 69504
H8773 H4784 BP337-500 BP151-500 Cat# M0314S Cat# 638909 Cat# 28706 Cat# 69504
H4784 BP337-500 BP151-500 Cat# M0314S Cat# 638909 Cat# 28706 Cat# 69504
BP337-500 BP151-500 Cat# M0314S Cat# 638909 Cat# 28706 Cat# 69504
BP151-500 Cat# M0314S Cat# 638909 Cat# 28706 Cat# 69504
Cat# M0314S Cat# 638909 Cat# 28706 Cat# 69504
Cat# 638909 Cat# 28706 Cat# 69504
Cat# 28706 Cat# 69504
Cat# 28706 Cat# 69504
Cat# 69504
Cat# P2075
2000 - 2010
Cat# 11093274910
S3771
Cat # NC1194374
Catalog # M0646M
Cat # AM1908
ory Stowers Original Data Repository: http://www. stowers.org/research/publications/libpb-2489
#1495
14026-0451.02
14023-0361.09
14024-0371.13
14011-0121.87
#38430
N/A
1 4/7 1
1971
NA





EXPERIMENTAL MODEL AND STUDY PARTICIPANT DETAILS

Drosophila strains

Stocks were obtained from both the National Drosophila Species Stock Center at Cornell (*D. eugracilis* 14026-0451.02), *D. biarmipes* (14023-0361.09), *D. ananassae* (14024-0371.13), *D. pseudoobscura* (14011-0121.87) the Bloomington Drosophila Stock Center: *D. melanogaster yellow white* (y¹w¹, Bloomington Stock Center #1495), UAS-ovoB on the chromosome II (Bloomington Stock Center #38430). Additionally, PoxN-Gal4 (Poxn-Gal4 construct #13 from Boll and Noll⁵¹) was a gift from the Noll lab.

METHOD DETAILS

Sample collection, dissection, and fixation

Male white pre-pupae were collected at room temperature and incubated in a petri dish containing a moistened Kimwipe at 25°C before dissection. After incubation, pupae were impaled in their anterior region and immobilized with forceps and placed in a glass dissecting well containing phosphate-buffered saline (PBS). The posterior tip of the pupa (20%–40% of pupal length) was separated and washed with a P200 pipette to flush the pupal terminalia into solution. Samples were then collected in PBS with 0.1% Triton-X-100 (PBT) and 4% paraformaldehyde (PFA, E.M.S. Scientific) on ice, and multiple samples were collected in the same tube. Samples were then fixed in PBT + 4% PFA at room temperature for 30 min, washed three times in PBT at room temperature, and stored at 4°C. At least 4 samples were imaged for each *in situ* hybridization probe and are available on Stowers Original Data Repository: http://www.stowers.org/research/publications/libpb-2489.

Probe design and synthesis

Templates for 200-300 base pair RNA probes were designed from a large exon present in all annotated isoforms of each examined gene. Exons were chosen by retrieving the decorated FASTA from flybase.org, ³⁴ and annotated isoforms were examined using the UCSC genome browser. ⁶⁰ After exon selection, Primer3Plus ⁶¹ was used to design PCR primers that would amplify a 200-300 base pair region, and 5-10 candidate primer pairs were screened using the UCSC In Silico PCR tool to identify sets that would amplify the region of interest from both *D. melanogaster* and *D. eugracilis*. This screening process was implemented to maximize the utility of any particular primer set for other species. Reverse primers were designed beginning with a T7 RNA polymerase binding sequence (TAATACGACTCACTATAG), and template DNA was PCR amplified from adult fly genomic DNA extracted using the DNeasy kit (-QIAGEN). Digoxigenin-labeled probes were then synthesized using in vitro transcription (T7 RNA Polymerase, Promega / Life Technologies), ethanol precipitated, and resuspended in water for Nanodrop analysis. Probes were stored at -20C in 50% formamide prior to *in situ* hybridization.

Antibody generation

The rabbit antibody for Shavenbaby (Svb) was produced by GenScript against the following amino acid sequence:

MHHHHHGGQSSMMGHPFYGGNPSAYGIILKDEPDIEYDEAKIDIGTFAQNIIQATMGSSGQFNASAYEDAIMSDLASSGQCPNGAVDPL QFTATLMLSSQTDHLLEQLSDAVDLSSFLQRSCVDDEESTSPRQDFELVSTPSLTPDSVTPVEQHNANTSQLDALHENLLTQLTHNMARN SSNQQQHHQQHNV.

DNA sequence

Bold indicates the start codon and His tag.

Italicized indicates the stop codon.

This sequence was cloned into the pET-30a (+) with His tag vector and transformed into *E. coli* strain BL21 StarTM (DE3). Transformants were induced with IPTG. The induced protein was purified via Ni column.

CRISPR

To induce mosaic knockouts⁵⁰ of *white* and *shavenbaby*, we targeted the first or second coding exon and ran the *D. eugracilis* and *D. melanogaster* sequences through the CRISPR Optimal Target Finder (http://targetfinder.flycrispr.neuro.brown.edu/)⁶² to avoid off-target effects. We generated our sgRNAs following the protocol outlined in Méndez-González et al.⁶³ 20 bp target-specific primers included the T7 promoter sequence (upstream) in the 5' end and overlapped with the sgRNA scaffold (see Table S4). Each target-specific primer was added with three primers for an overlap extension PCR generating a 130 bp DNA template. The PCR reaction was then used as a template for in vitro transcription using EnGen sgRNA Synthesis Kit (NEB), and the MEGACLEAR Transcription

Current Biology Article



Clean-Up KIT (Invitrogen) was used to purify the sgRNA product. CRISPR-Cas9 injections were performed in-house following standard protocols (http://gompel.org/methods). We used an injection mix containing two (white control) or four (white shavenbaby experimental) sgRNAs targeting the first or second exon (100 ng/µl) and CAS9 protein (EnGen Spy Cas9 NLS from NEB, Catalog # M0646M). PCR amplification and sanger sequencing of the regions around the predicted sgRNA targets for 2 individuals were used to confirm that our injections induced the desired mutations. Individuals shavenbaby white #36 and #51, which were injected with shavenbaby sgRNAs 1,2 and white sgRNAs 3,4 (see Figure S9), both show sequence variation around the predicted cut sites in DNA extracted from whole bodies minus the genitalia.

Imaging

After fixation, the developing pupal genitalia of *D. melanogaster* and *D. eugracilis* were stained with rat anti-E-cadherin, 1:100 in PBT (DSHB Cat# DCAD2, RRID:AB_528120) overnight at 4°C, followed by an overnight at 4°C incubation with anti-rat 488, 1:200 (Invitrogen) to visualize apical cell junctions while, Rho-phalloidin (Invitrogen, Catalog # R415), 1:100, was used to visualize actin, *shaven-baby* 1:10 with anti-rabbit 488, 1:200 (Invitrogen) in the genitalia and 1:50 with anti-rabbit 568, 1:500 (Invitrogen) for the embryo.

Fluorescently labeled samples were mounted in glycerol mounting solution (80% glycerol, 0.1 M Tris, pH 8.0) on microscope slides coated with poly-L-lysine (Thermo Fisher Scientific #86010). Samples were imaged at ×40 on a Leica TCS SP8 confocal microscope. We used the MorphoGraphX software package⁶⁴ to render images in three dimensions. This allowed us to rotate the samples to better present the most informative perspectives of the various phallic structures.

We used an InsituPro VSi robot to perform *in situ* hybridization following the protocol of Vincent et al.⁶⁵ Briefly, dissected terminalia were rehydrated in PBT, fixed in PBT with 4% PFA, and prehybridized in hybridization buffer for 1 hr at 60C. Samples were then incubated with probes for 16h at 60C before being washed with hybridization buffer followed by PBT. Samples were incubated in PBT block (1% bovine serum albumin) for 2 hr. Samples were then incubated with anti-digoxigenin Fab fragments conjugated to alkaline phosphatase (Roche) diluted 1:6000 in PBT+BSA. After additional washes, color reactions were performed by incubating samples with NBT and BCIP (Promega) until a purple stain could be detected under a dissecting microscope. Samples were mounted in glycerol on microscope slides coated with poly-L-lysine and imaged at 20X or 40X magnification on a Leica DM 2000 with a Leica DFC450C camera using the ImageBuilder module of the Leica Application Suite.

For light microscopy of adult phallic microdissections, samples were mounted in PVA Mounting Medium (BioQuip) until fully cleared or with glycerol mount. They were then imaged at ×20 magnification on a Leica DM 2000 with a Leica DFC450C camera using the ImageBuilder module of the Leica Application Suite.

QUANTIFICATION AND STATISTICAL ANALYSIS

The distribution of the major trichome height for the *white* control was normal (Shapiro-Wilk normality test W = 0.9637, p-value = 0.1788), allowing us to infer outlier major trichome height in the *white shavenbaby* experimental data. We used -3SD below control white major trichome height as our significance cutoff, as values below this number should occur at a rate of 0.15% with a normal distribution. For our 54 samples of *white shavenbaby* experimental data, we would expect to see 0.081 data points below this value if the CRISPR sgRNAs do not affect the major trichome height.